Thermal Physics and Glaucoma II: Preliminary Evidences for a Thermophysical Design of a Possible Visible-Light-Photons Therapy

Giulia Grisolia [1,*], Mariarosa Astori [2], Antonio Ponzetto [3], Antonio Vercesi [4] and Umberto Lucia [1,*]

[1] Dipartimento Energia "Galileo Ferraris", Politecnico di Torino, Corso Duca Degli Abruzzi 24, 10129 Torino, Italy

[2] Dipartimento di Oculistica, Azienda Ospedaliera Nazionale "SS. Antonio e Biagio e Cesare Arrigo", Via Venezia 7, 15121 Alessandria, Italy; mrastori@ospedale.al.it

[3] Department of Medical Sciences, University of Torino, Corso A.M. Dogliotti 14, 10126 Torino, Italy; antonio.ponzetto@unito.it

[4] Studio Oculistico A. Vercesi, Via Massa Saluzzo 20, 15057 Tortona (AL), Italy; info@studiovercesi.it

[*] Correspondence: giulia.grisolia@polito.it (G.G.); umberto.lucia@polito.it (U.L.); Tel.: +39-011-090-4558 (G.G.)

Abstract: Recently, a non-equilibrium thermodynamic approach has been developed in order to model the fundamental role of the membrane electric potential in the cell behaviour. A related new viewpoint is introduced, with a design of a photobiomodulation treatment in order to restore part of the visual field. Here, a first step in experimental evidence of the validity of the thermodynamic approach is developed. This result represents the starting point for future experimental improvements for light stimulation in order to improve the quality of life of the patients. The future possible therapy will be in addition to the pharmacological treatments.

Keywords: photobiomodulation; glaucoma; non-equilibrium thermodynamics; ions fluxes; transport theory; thermodynamics of bio-systems

1. Introduction

Glaucoma is an ophthalmic disease that affects around 1% of people aged over 40 years, 5% of people aged 70 years and older, and 10% of those older than 80 years [1], and it can lead to irreversible blindness. The studies on the glaucoma diffusion in the next years show that 112 million of people are expected to loose their vision by 2040 [1,2].

The open-angle glaucoma is the most widespread type of this disease, and it is related to the ocular hypertension which causes an impairment of retinal ganglion axons cells [3–7], which make up the optical nerve, resulting in a progressive loss of retinal ganglion cells [8–10]. At present, the clinical treatments are aimed at lowering the intraocular pressure with the intent of increasing the duration of patients vision. However, vision is not only related to eyes. Indeed, it is the result of a complex information processing that occurs in the brain. Thus, to treat damage to it, a holistic approach is needed to support the actual treatments [11], improving the reduced information flow that reaches the brain [12–14], optimising the entire process.

Recently, a thermodynamic approach to glaucoma and a thermophysical model the optic nerve behaviour have been developed [15]: the thermodynamic analysis pointed out the possible modification of the behaviour of the optical nerve by changing in the membrane electric potential.

Moreover, the thermophysical results highlighted also that a control of the membrane electric potential could produce regeneration, because the supply of energy generates ion fluxes, with a consequent change in the membrane electric potential.

Consequently, we argued that a possible way to supply energy could be the use of visible light [15], in relation to the recent evidences that photostimulation can promote

regeneration and functionality after nerve injury [16–18], and to the experimental and clinical results of the effect of a non-thermal low dose light emitting diode (LED) array on human cells [19,20]. Indeed, electrical activity has a fundamental role in stimulating the regrowth potential of the central nervous system neurons [21,22].

However, these theoretical results have been only a possible hypothesis of new complementary therapies. So, an experimental approach has been developed, to obtain evidence, in order to design a new visible light complementary therapy for glaucoma. Indeed, photostimulation has just been used in neuromodulation [23]: neural stem cells have been shown to express blue/red light-sensitive photoreceptors [24]. Moreover, the proliferation and regulation of neural stem cells to neuronal or glial cells are wavelength-specific; indeed, low-power (300 µW cm^{-1}) monochromatic blue light (455 nm wavelength) was shown to increase astrocyte differentiation. The behaviour of the neurones of the central nervous system depends on mitochondrial generated ATP, and four major mitochondrial protein complexes related to the generation of ATP present interaction with light of different wavelengths [25].

So, in this paper we summarise a first experimental approach to evaluate the use of visible light as a possible support to contrast glaucoma, as the thermophysical model suggests. The results obtained represent a new viewpoint to introduce the visible light as a support to the pharmacological therapies, in order to improve the quality of life of the patients.

2. Materials and Methods

In this paper, we summarise the experimental confirmation of the results obtained from the thermodynamic approach [15]. To do so, we first summarise the previous thermodynamic results and, then, describe the experimental approach used.

The living cell membrane is characterised by an electric potential difference $\Delta\phi$ between the cytoplasm and the extracellular environment, with reference to the environment [26]. This membrane electric potential is related to different permeabilities of some ions (Na$^+$, K$^+$, Cl$^-$, Ca^{2+}, etc.). Let us consider the differential of the Gibbs free energy G [27–29]:

$$dG = V\,dp - S\,dT + \sum_i \mu_i\,dN_i \tag{1}$$

where V is the volume of the system considered, S is the entropy, μ_i represents the chemical potential of the i-th chemical species, and N stands for the number of particles which flow across the boundary of the system. In relation to the distributions of the different ions, there exists an electric potential differences. In particular, cations (ions with positive charge) accumulate in low electric potential energy regions, while anions (ions with negative charges) present higher concentration at high values of electric potential energy regions [30]. The ion concentrations can be expressed as follows [30]

$$c_N = c_{N,0} \exp\left(\frac{N\,e_N}{k_B\,T}\right) \tag{2}$$

where c_N is the concentrations related to the number of molecules, e_N is the energy per molecule, k_B (= 1.38×10^{-23} J K^{-1}) is the Boltzmann constant, T is the temperature, c_{N0} is the reference value of c_N at $e_N = 0$ J molecule^{-1}, and $k_B T \approx 4 \times 10^{-21}$ J molecule^{-1} for ordinary temperature [30]. The electric potential can be evaluated by using the Goldman–Hodgkin–Katz equation [27,30]:

$$\Delta\phi = \frac{R\,T}{F}\,\log_{10}\left(\frac{P_{\text{Na}^+}\,[\text{Na}^+]_{\text{out}} + P_{\text{K}^+}\,[\text{K}^+]_{\text{out}} + P_{\text{Cl}^-}\,[\text{Cl}^-]_{\text{out}}}{P_{\text{Na}^+}\,[\text{Na}^+]_{\text{in}} + P_{\text{K}^+}\,[\text{K}^+]_{\text{in}} + P_{\text{Cl}^-}\,[\text{Cl}^-]_{\text{in}}}\right) \tag{3}$$

where P is the permeability of the ion, [A] means concentration of the A-ion, R is the ideal gas constant, T is the temperature, F is the Faraday constant, and out stand for

outside, while in for inside. This last relation points out how the membrane potential can be changed by alterations in the conductance of one or more ion. The ion channels and transporters provide different permeability to distinct ions, such as Na^+, K^+, and Cl^-.

Any change in the ion concentration changes both the membrane electric potential and the related pH of the cytoplasm, because the concentration of a chemical species and the pH can be obtained by the following relations [27,30]:

$$c_{out} = c_{in} \exp\left(\frac{\Delta\phi}{R\,T}\right) \tag{4}$$

and

$$\Delta\phi = \Delta G_{H^+} + 2.3\,\frac{R\,T}{F}\,\Delta pH \tag{5}$$

where G is the Gibbs potential, F is the Faraday constant, $2.3\,\Delta pH$ is the physiological concentration gradient, and H^+ is the Hydrogen ion which is used by the cells in order to modulate the membrane electric potential by changing the H^+ concentration. These changes in the ion transport modify the biochemical reactions inside the cells (the optic nerve in our analysis), with related modifications of the biochemical processes. Indeed, proteins play a fundamental role in ion transport. Proteins in the cytosol can be modified in their functions by phosphorylation or dephosphorylation. An ion actively crosses the membrane against its electrochemical potential, whereby the necessary energy is derived either from the hydrolysis of ATP, or from the movement of a co-transported, or coupled ion along its electrochemical gradient. In this context, the role played by the H^+-ATPase is fundamental, because it moves positive charges into the cell, while it generates large membrane voltage (inside negative and outside positive) and a pH gradient [30–33]. Protein phosphorylation is an important cellular regulatory mechanism, because many enzymes and receptors [28,34,35] are activated or deactivated by phosphorylation by involving kinases and phosphatases. Moreover, kinases are responsible for cellular transduction signalling [7,36–38]. When ion fluxes occur, a variation in the concentration of the ions on both side of the membrane occurs [39,40]:

$$\frac{dc_i}{dt} = -\nabla \cdot \mathbf{J}_i \tag{6}$$

where c_i is the concentration of the i-th ion (Na^+, K^+, Ca^{2+}, Cl^-, etc.) in $C\,m^{-3}$, t is the time and $\mathbf{J}_i$ is the current density of the i-th ion. However, as a consequence of these cellular fluxes and processes, a specific entropy rate is generated [41,42]:

$$T\,\frac{ds}{dt} = \nabla \cdot \left(\mathbf{J}_u - \sum_{i=1}^{3} \mu_i\,\mathbf{J}_i\right) - \sum_{i=1}^{3} \mathbf{J}_i \cdot \nabla\mu_i \tag{7}$$

where s is the specific entropy, T is the temperature, $\mathbf{J}_S = \mathbf{J}_u - \sum_{i=1}^{3} \mu_i\,\mathbf{J}_i$ is the contribution of the inflows and outflows, with $i = 1, 2, 3$ meaning Cl^--, Na^+-, K^+-fluxes, $T\sigma = -\sum_{i=1}^{3} \mathbf{J}_i \cdot \nabla\mu_i$ is the dissipation function [40], and μ is the chemical potential, defined as:

$$\mu_i = \left(\frac{\partial G}{\partial n_i}\right)_{T,p,n_{k \neq i}} \tag{8}$$

where G is the Gibbs energy, n is the number of moles, and p is the pressure.

In relation to the ion fluxes, we also wrote the Equation (7) in a different way [15]:

$$T\,\frac{ds}{dt} = -\nabla \cdot \left(\mathbf{J}_u - \sum_{i=1}^{3} \mu_i\,\mathbf{J}_i\right) \tag{9}$$

which, considering T constant and following Prigogine ($ds/dt = 0$) [43], becomes:

$$\nabla \cdot \left(\mathbf{J}_u - \sum_{i=1}^{3} \mu_i \mathbf{J}_i \right) = 0 \qquad (10)$$

So, taking into account the change in the internal energy, we obtained [15]:

$$\int_V \frac{du}{dt} dV = - \int_V \nabla \cdot \mathbf{J}_u dV = \dot{Q} \qquad (11)$$

where u is the specific internal energy, $\mathbf{J}_u$ is the heat flux in W m^{-2}, V is the cell volume in m^3, and $\dot{Q}$ is the heat power in W, represented also by the power of the electromagnetic waves flowing into the eyes.

Now, we describe the following experimental approach.

In chronic glaucoma, the Retinal Nerve Fibre Layer (RNFL) tends to gradually reduce, until the connection between the retina and the nervous system disappears. Indeed, the first glaucomatous lesions seem to occur in the brain, and they are quite similar to other neurodegenerative diseases lesions. The nervous system also reacts by processing a compensatory response to maintain the signal between the eye and brain regions, slowing the progression of the disease, which can be interpreted as a balance between the disease and a brain adaptation. Moreover, recently, some degree of regeneration has been achieved by the optic nerve by factors associated with intraocular inflammation, as our thermodynamic model suggests. So, in relation to Equations (1) and (6), specific energy fluxes could allow the retinal ganglion cells to regenerate axons, from the eye through the entire length of the optic nerve. Progress in optic nerve regeneration holds promise for visual restoration [44,45]. Indeed, retinal ganglion cell activity has been shown to increase, if stimulated by visual stimulation, with a consequent axons regeneration, due to the neural activity [21,46]. Consequently, the rationale of our analysis consists in verifying the effectiveness of the visible light phototherapy in relation to rehabilitation. The stimulating system is based on the stimulation of the above mechanism, in order to keep the optic nerve signal alive, avoiding or reducing the neurochemical phenomena related to ocular nervous fibres degeneration of the fibres of the ocular nerve. Therefore, we could consider effective the light stimulation if a slowing in the progression of the disease occurs, and the visual field, and the quality of vision, is maintained or improved.

In order to obtain experimental evidence in relation to our thermodynamic results, useful for the definition of a more detailed trial on a large number of patients, and to design a possible future therapy, we have developed a first trial on a small set of patients, approved by our bio-ethic board. So, this operative study is focused on the achievement of two objectives specific for patients with pathologies concerning damage to the optic nerve resulting from primary chronic open-angle glaucoma:

- Primary objective: to verify a reduction in the damage to the optic nerve, and a progressive recovery of vision, in patients undergoing rehabilitation therapy, based on visual stimuli;
- Secondary objective: to verify an improvement in the quality of life in enrolled patients.

The criteria to enrol the patients can be summarised as follows:

- They are affected by a chronic open angle glaucoma;
- The damage is no more than the 50% of the vision field;
- They do not suffer any further disease.

The number of patients suggested by the bio-ethic board was twelve white Italians, as reported in Table 1. All the patients enrolled continued their pharmacological treatments. All the patients were enrolled after an ophthalmic visit and anamnesis of vision loss in certain areas.

Table 1. Patients enrolled by age and gender.

| Patient	Age	Gender
1	54	male
2	59	male
3	53	female
4	47	male
5	55	female
6	59	female
7	58	female
8	74	female
9	73	female
10	49	female
11	52	male
12	72	female

The quantitative technical diagnosis was obtained using Optic Computed Tomography (OCT). OCT is an imaging technique that uses low-coherence (or white light) interferometry to capture micrometer resolution, from within optical scattering media [47]. Ocular OCT is used by ophthalmologists to obtain high-resolution images of the retina and anterior segment [48]. It provides a straightforward method of assessing cellular organisation, photoreceptor integrity, and axonal thickness in glaucoma, macular degeneration, retinal nerve fibre layers (RNFL), etc. Since 1991, OCT has been improved by rapid evolution for use in detection and monitoring of glaucoma and macular diseases. Indeed, average RNFL thickness indicates patient overall RNFL health. The mean value for RNFL thickness in the general population is 92.9 ± 9.4 μm [49–53]. Typically, a normal, non-glaucomatous eye has an RNFL thickness of 80 μm or greater, and is represented by green colour in the OCT exam result. An eye with an average RNFL thickness of 70 μm to 79 μm is suspected of glaucoma, and is represented by yellow colour in the OCT exam result. OCT shows optic nerve hypoplasia (ONH) and RNFL parameters: RNFL and ONH parameters present a green colour code for normality, values below normality present a red colour code, and borderline values are represented by a yellow colour code. A white colour code refers to values above the normality range, and grey indicates that normative data are not applicable. Red colour represents the diseased thickness.

All the patients undergo an optical computed tomography CIRRUS 5000 by Carl Zeiss (Oberkochen, Germany) scan prior to and after the complementary therapy.

The treatment is realised by using the smartphones of the patients (Android OS, display Touchscreen, 6.3 in, pixels 2340×1080). Python-based software generates the stimuli on the patient's smartphone screen. The software generates light circles which move randomly around the periphery of the area of visual loss: this is the treatment suggested. So, the moving circles appear on the screen, upon which the patients gaze must remain fixed. In summary, the treatment is realised by mapping the screen by coloured circles, around the border of the visual loss area, as represented in Figure 1. A personalised set of moving lights is generated for each patient at each point of the therapeutical procedure.

There are no problems regarding infrared or ultraviolet stimuli, because the screen is CE-certificated and used worldwide by every smartphone owner. The lightness of the screen of the smartphone was set at 50%. Moreover, the energy of the stimuli cannot produce any damage to the cornea of the retina of the patients, as certified by the CE certification for smartphone use.

The stimulation is performed for ten minutes a day, only for the treated eye. The treatment is applied every day in a month for five months. The patients apply their therapy at home. Each month, they are controlled by the ophthalmologist, in order to evaluate any possible difficulty or improvement. No patient complained of difficulties during the therapy.
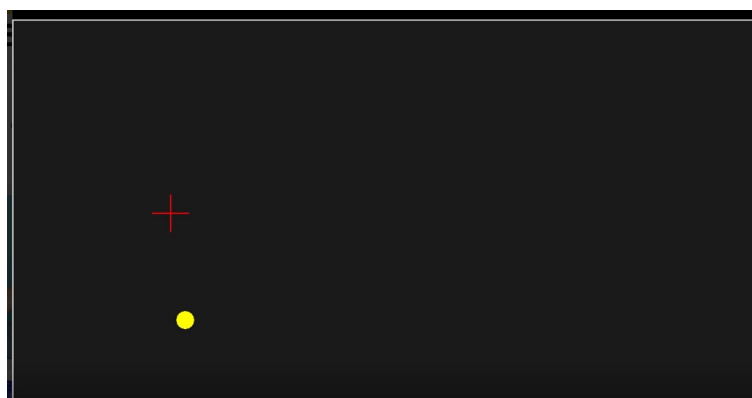
Figure 1. An example of treatment. Coloured circles map the screen at the border of the visual field lost.

The colours were defined in relation to the analysis of the visual deficit in relation to vision perception [54]. The colours used were generated using the following table (Table 2).

Table 2. Table of colours used during the therapy.

| Wavelength (nm)	sRGB	Hex Triplet
491.41	(0,255,255)	#00ffff
497.49	(207,52,118)	#cf3476
549.13	(255,0,255)	#ff00ff
570.47	(255,255,0)	#ffff00

The circles map the screen corresponding to the periphery of the visual field lost (in the transition zone [55,56], the region at the border between the damaged and non-damaged visual field sector).

3. Results

In this section, we wish to highlight the results obtained by only analysing a patient. So, in Figure 2A,B, we show an example of regeneration of the treated area, as observed, for an Italian white male patient aged 54, affected by bilateral open angle glaucoma, more severe on the left eye, since he was 45. Moreover, the patient has no other pathology and he is treated with timolol (twice a day) and dorzolamide (three times a day). All the patients reported an improvement of the visual sensation with particular reference to the recovery of depth. In Figure 2, the OCT of this patient is represented as an example. We can highlight that:

- In relation to nerve fibre layer, the thickness map is a topographical display of RNFL, an hourglass shape of yellow and red colours, typical of normal eyes. In relation to this patient, we can observe a reduction in nerve fibre in the exam of March 2020, but an improvement in the exam in July 2020;
- The key parameters in the table show average RNFL thickness for the patient: in March 2020 the right eye measured 55 μm and the left eye measured 44 μm, while in July 2020 the right eye measured 64 μm and the left eye 44 μm;
- RNFL quadrant and clock hour: characteristic parameters are temporal, superior, nasal, and inferior quadrants; in relation to the patient considered, we can highlight:
  - In March 2020: the right eye presents a reduction in fibres in the superior, nasal and inferior quadrant, and normal values in the temporal quadrant, while the left eye presents a reduction in fibres in all quadrants;
  - In July 2020: the right eye presents an improvement of fibres in the damaged areas, in particular in the nasal and inferior quadrants, a smaller improvement in the superior quadrant, and unchanged fibres in the temporal quadrant, while the

left eye presents an improvement in the nasal quadrant, an unchanged number of fibres in the superior and temporal quadrant, but a reduction in fibres in the temporal quadrant.
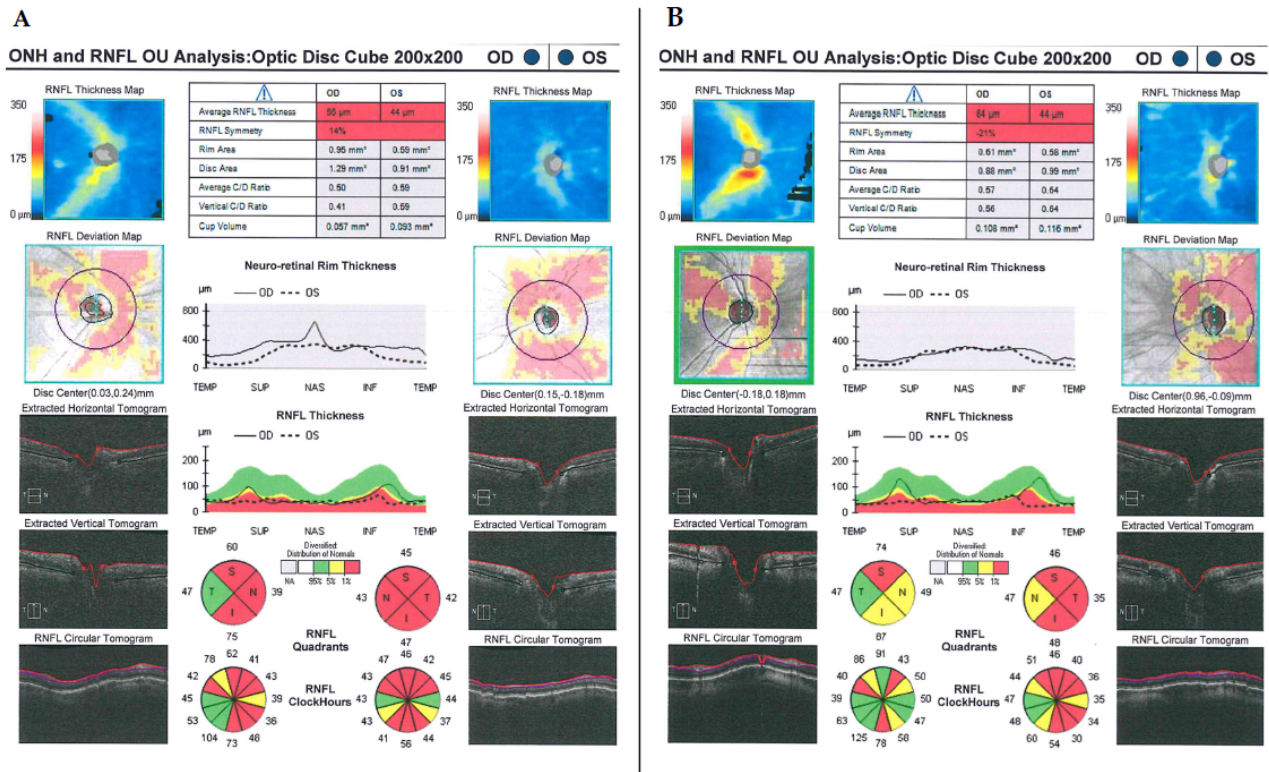
Figure 2. Example of the effect of the experimental light stimulation, as designed by the thermophysical approach. The patient is a 54-year-old man with glaucoma since he was 45, without any other pathology. The patient has been treated for 5 months, ten minutes per day everyday during any month, for each eye. The optical tomography of a patient before the treatment (**A**) and after the treatment (**B**). It is possible to highlight an improvement in the Nerve Fibre Layer. OS means Left Eye. OD means Right Eye. The colour scheme in the OCT is defined as follows: green colour code represents normality, yellow represents the suffering state and red represents the damaged state. The OCT system used has been the Zeiss CIRRUS 5000.

The results here summarised represent a starting point for a further experimental analysis, but it is needed to highlight an experimental evidence for the confirmation of the thermodynamic results and the design of a possible photobiomodulation complementary light therapy for glaucoma.

4. Discussion and Conclusions

Blue light (400–480 nm) has been shown to affect flavin and cytochrome constituents associated with mitochondria, and to decrease the rate of ATP formation, with a related production of ROS and cell death [25]. On the contrary, red light (650–800 nm) has been shown to affect mitochondrial complex IV or cytochrome oxidase, and to increase the rate of formation of ATP, with a related generation of a number of beneficial factors [25].

The thermodynamic approach highlights that external stimuli can induce continuous metabolic generation, characterised by a relation between the ion fluxes and heat power density generated. Indeed, it has been shown a relation between photobiomodulation and nerve regeneration, with a related increase in the number of myelinated fibres and an improvement of electrophysiological function, leading to the conclusion that beneficial effects occur in relation to the recovery of nerve lesions [16].

So, a possible approach could be related to visible light stimulation. In order to generate the appropriate stimuli, we referred to the results obtained in the analysis of optimal

vision perception [54,57], which lead to the frequencies summarised in Table 2. Indeed, they appear the frequencies related to the spontaneous optimisation of the biological processes for vision, as discussed in Ref. [58]. These experimental results follow the same approach as our theoretical one, which is based on optimisation theory in engineering thermodynamics [43,59]. In this paper, we summarise the results obtained by a first experimental proof in order to point out the effect of the visible light, if used in subsequent monochromatic stimulations.

The results obtained open the way to future trials in order to design a therapeutical device for the glaucoma treatment to be considered in addition to the pharmacological treatments, in order to improve the quality of life of the patients.

This paper is a communication, so it represents a starting point for future deeper analyses of the present experimental evidence, which represent preliminary results that must be improved on considering a larger set of patients. So, we think that, after an improvement of this evidence by a more detailed experimental analysis which will be developed in the next future six months, and the results will be statistically significant and will point out improvement in clinical examinations, then this approach could be considered for possible use in the clinical treatments for glaucomatous patients, in order to support the drug therapies for an improvement of the vision restoration of the patients, and a consequent their well-being.

5. Patents

Patent No. 102019000012687 dated 23 July 2019: "Dispositivo e Metodo per la Riabilitazione Visiva"; owner: Politecnico di Torino (Italy).

Author Contributions: Conceptualisation, U.L. and G.G.; methodology, U.L., A.P. and G.G.; validation, M.A., A.P. and A.V.; formal analysis, U.L. and G.G.; investigation, U.L. and G.G.; resources, U.L.; data curation, M.A. and A.V.; writing—original draft preparation, U.L. and G.G.; writing—review and editing, U.L. and G.G.; visualisation, M.A., A.P. and A.V.; supervision, U.L. and A.P.; project administration, U.L.; funding acquisition, U.L. All authors have read and agreed to the published version of the manuscript.

Institutional Review Board Statement: The study was conducted according to the guidelines of the Declaration of Helsinki, and approved by the Ethics Committee Comitato Etico Interaziendale AUO Città della Salute e della Scienza di Torino, AO Ordine Mauriziano di Torino (Prot.n. 0010358, 1 February 2021, Titolario A2.4.8, Pratica n. 385/2020).

Informed Consent Statement: Informed consent was obtained from all subjects involved in the study.

Data Availability Statement: The data reported in this paper are retained by the Azienda Ospedaliera "SS. Antonio e Biagio e Cesare Arrigo" (Alessandria) and by the Studio Oculistico A. Vercesi (Tortona-AL), in accordance to the Italian Law on privacy for Health System. The data can be required by a formal request to Dott. M. Astori and Dott. A. Vercesi.

Conflicts of Interest: The authors declare no conflict of interest, a part the patent declared in Section 5.

References

1. Parsadaniantz, S.M.; le Goazigo, A.R.; Sapienza, A.; Habas, C.; Baudouin, C. Glaucoma: A Degenerative Optic Neuropathy Related to Neuroinflammation? *Cells* **2020**, *9*, 535. [CrossRef] [PubMed]
2. Quigley, H.A.; Broman, A.T. The number of people with glaucoma worldwide in 2010 and 2020. *Br. J. Ophthalmol.* **2006**, *90*, 262–267. [CrossRef] [PubMed]

3. Do, M.; Yau, K. Intrinsically Photosensitive Retinal Ganglion Cells. *Physiol. Rev.* **2010**, *90*, 1547–1581. [CrossRef]
4. Martucci, A.; Cesareo, M.; Napoli, D.; Sorge, R.; Ricci, F.; Mancino, R.; Nucci, C. Evaluation of pupillary response to light in patientswith glaucoma: a study using computerized pupillometry. *Int. Ophthalmol.* **2014**, *34*, 1241–1247. [CrossRef]
5. Garhöfer, G.; Zawinka, C.; Resch, H.; Huemer, K.; Schmetterer, L.; Dorner, G. Response of Retinal Vessel Diameters to Flicker Stimulation in Patients with Early Open Angle Glaucoma. *J. Glaucoma* **2004**, *13*, 340–344. [CrossRef]
6. Ofri, R.; Narfström, K. Light at the end of the tunnel? Advances in the understanding and treatment of glaucoma and inherited retinal degeneration. *Vet. J.* **2007**, *174*, 10–22. [CrossRef]
7. Lucia, U.; Grisolia, G.; Francia, S.; Astori, M.R. Theoretical biophysical approach to cross-linking effects on eyes pressure. *Phys. A* **2019**, *534*, 122163. [CrossRef]
8. Gupta, N.; Yücel, Y. Glaucoma as a neurodegenerative disease. *Curr. Opin. Ophthalmol.* **2007**, *18*, 110–114. [CrossRef] [PubMed]
9. Mesentier-Louro, L.; Liao, Y. Optic Nerve Regeneration: Considerations on Treatment of Acute Optic Neuropathy and End-Stage Disease. *Curr. Ophtalmol. Rep.* **2019**, *7*, 11–20. [CrossRef]
10. de Zavalía, N.; Plano, S.A.; Fernandez, D.C.; Lanzani, M.F.; Salido, E.; Belforte, N.; Sarmiento, M.I.K.; Golombek, D.A.; Rosenstein, R.E. Effect of experimental glaucoma on the non-image forming visual system. *J. Neurochem.* **2011**, *117*, 904–914. [CrossRef] [PubMed]
11. Sabel, B.; Cárdenas-Morales, L.; Gao, Y. Vision Restoration in Glaucoma by Activating Residual Vision with a Holistic, Clinical Approach: A Review. *J. Curr. Glaucoma Pract.* **2011**, *12*, 1–9. [CrossRef] [PubMed]
12. Sabel, B.; Kasten, E. Restoration of vision by training of residual functions. *Curr. Opin. Ophthalmol.* **2000**, *11*, 430–436. [CrossRef] [PubMed]
13. Jutley, G.; Luk, S.; Dehabadi, M.; Cordeiro, M. Management of glaucoma as a neurodegenerative disease. *Neurodegener. Dis. Manag.* **2017**, *7*, 157–172. [CrossRef] [PubMed]
14. Jobke, S.; Kasten, E.; Sabel, B. Vision Restoration Through Extrastriate Stimulation in Patients With Visual Field Defects: A Double-Blind and Randomized Experimental Study. *Neurorehabilit. Neural Repair* **2009**, *23*, 246–255. [CrossRef]
15. Lucia, U.; Grisolia, G. Thermal Physics and Glaucoma: From Thermodynamic to Biophysical Considerations to Designing Future Therapies. *Appl. Sci.* **2020**, *10*, 7071. [CrossRef]
16. de Oliveira Rosso, M.P.; Buchaim, D.V.; Kawano, N.; Furlanette, G.; Pomini, K.T.; Buchaim, R.L. Photobiomodulation Therapy (PBMT) in Peripheral Nerve Regeneration: A Systematic Review. *Bioengineering* **2018**, *5*, 44. [CrossRef]
17. Sabel, B.; Henrich-Noack, P.; Fedorov, A.; Gall, C. Chapter 13—Vision restoration after brain and retina damage: The "residual vision activation theory". In *Enhancing Performance for Action and Perception*; Green, A., Chapman, C., Kalaska, J., Lepore, F., Eds.; Elsevier: Amsterdam, The Netherlands, 2011; Volume 192, pp. 199–262. [CrossRef]
18. Yang, S.G.; Li, C.P.; Peng, X.Q.; Teng, Z.Q.; Liu, C.M.; Zhou, F.Q. Strategies to Promote Long-Distance Optic Nerve Regeneration. *Front. Cell. Neurosci.* **2020**, *14*, 119. [CrossRef] [PubMed]
19. Weiss, R.A.; McDaniel, D.H.; Geronemus, R.G.; Weiss, M.A. Clinical Trial of a Novel Non-Thermal LED Array for Reversal of Photoaging: Clinical, Histologic, and Surface Profilometric Results. *Lasers Surg. Med.* **2005**, *36*, 85–91. [CrossRef] [PubMed]
20. McDaniel, D.H.; Weiss, R.A.; Geronemus, R.G.; Mazur, C.; Wilson, S.; Weiss, M.A. Varying Ratios of Wavelengths in Dual Wavelength LED Photomodulation Alters Gene Expression Profiles in Human Skin Fibroblasts. *Lasers Surg. Med.* **2010**, *42*, 540–545. [CrossRef]
21. Lim, J.H.; Stafford, B.; Nguyen, P.; Lien, B.; Wang, C.; Zukor, K.; He, Z.; Huberman, A. Neural activity promotes long-distance, target-specific regeneration of adult retinal axons. *Nat. Neurosci.* **2016**, *19*, 1073–1084. [CrossRef]
22. Nuzzi, R.; Tridico, F. Glaucoma: Biological Trabecular and Neuroretinal Pathology with Perspectives of Therapy Innovation and Preventive Diagnosis. *Front. Neurosci.* **2017**, *11*, 494. [CrossRef]
23. Zimmerman, J.F.; Tian, B. Nongenetic optical methods for measuring and modulating neuronal response. *ACS Nano* **2018**, *12*. [CrossRef]
24. Wang, M.; Xu, Z.; Liu, Q.; Sun, W.; Jiang, B.; Yang, K.; Li, J.; Gong, Y.; Liu, Q.; Liu, D.; et al. Nongenetic optical modulation of neural stem cell proliferation and neuronal/glial differentiation. *Biomaterials* **2019**, *225*. [CrossRef]
25. Osborne, N.; Núnez-Álvarez, C.; del Olmo-Aguado, S.; Merrayo-Lloves, J. Visual light effects on mitochondria: The potential implications in relation to glaucoma. *Mitochondrion* **2017**, *36*. [CrossRef] [PubMed]
26. Yang, M.; Brackenbury, W.J. Membrane potential and cancer progression. *Front. Physiol.* **2013**, *4*, 185. [CrossRef] [PubMed]
27. Atkins, P.; Paula, J.D. *Physical Chemistry Life Science*; Oxford University Press: New York, NY, USA, 2006.
28. Lucia, U.; Grisolia, G. Thermal Resonance and Cell Behavior. *Entropy* **2020**, *22*, 774. [CrossRef] [PubMed]
29. Lucia, U.; Grisolia, G. Resonance in thermal fluxes through cancer membrane. *Atti dell'Accad. Peloritana Pericolanti* **2020**, *98*, 1–6. [CrossRef]
30. Ashrafuzzaman, M.; Tuszynski, J. *Membrane Biophysics*; Springer: Berlin/Heidelberg, Germany, 2013.
31. Nakanishi-Matsui, M.; Sekiya, M.; Futai, R.K.N.M. The mechanism of rotating proton pumping ATPases. *BBA-Bioenergetics* **2010**, *1797*, 1343–1352. [CrossRef] [PubMed]
32. Stevens, T.H.; Forgac, M. Structure, function and regulation of the vacuolar (H^+)-ATPase. *Annu. Rev. Cell. Dev. Biol.* **1997**, *13*, 779–808. [CrossRef] [PubMed]
33. Lucia, U.; Ponzetto, A.; Deisboeck, T.S. A thermo-physical analysis of the proton pump vacuolar-ATPase: The constructal approach. *Sci. Rep.* **2014**, *4*, 1. [CrossRef]

34. Rudolph, M.G.; Stanfield, R.L.; Wilson, I.A. How TCRs bind MHCs, peptides, and coreceptors. *Annu. Rev. Immunol.* **2006**, *24*, 419–466. [CrossRef]
35. Strong, R.K. Asymmetric ligand recognition by the activating natural killer cell receptor NKG2D, a symmetric homodimer. *Mol. Immunol.* **2002**, *38*, 1029–1037. [CrossRef]
36. Ardito, F.; Giuliani, M.; Perrone, D.; Troiano, G.; Muzio, L.L. The crucial role of protein phosphorylation in cell signaling and its use as targeted therapy. *Int. J. Mol. Med.* **2017**, *40*, 271–280. [CrossRef]
37. Lucia, U.; Grisolia, G.; Dolcino, D.; Astori, M.R.; Massa, E.; Ponzetto, A. Constructal approach to bio-engineering: the ocular anterior chamber temperature. *Sci. Rep.* **2016**, *6*, 31099. [CrossRef]
38. Lucia, U.; Grisolia, G.; Astori, M.R. Constructal law analysis of $Cl^−$ transport in eyes aqueous humor. *Sci. Rep.* **2017**, *7*, 6856. [CrossRef]
39. Callen, H.B. *Thermodynamics*; Wiley: New York, NY, USA, 1960.
40. Yourgrau, W.; van der Merwe, A.; Raw, G. *Treatise on Irreversible and Statistical Thermophysics*; Dover: New York, NY, USA, 1982.
41. Lucia, U.; Grisolia, G. How Life Works—A Continuous Seebeck-Peltier Transition in Cell Membrane? *Entropy* **2020**, *22*, 960. [CrossRef] [PubMed]
42. Lucia, U.; Grisolia, G. Non-equilibrium thermodynamic approach to Ca^{2+}-fluxes in cancer. *Appl. Sci.* **2020**, *10*, 6737. [CrossRef]
43. Prigogine, I. Structure, Dissipation and Life. In *Theoretical Physics and Biology*; Marois, M., Ed.; North Holland Pub. Co.: Amsterdam, The Netherlands, 1969.
44. Benowitz, L.I.; He, Z.; Goldberg, J.L. Reaching the brain: Advances in optic nerve regeneration. *Exp. Neurol.* **2017**, *287*, 365–373. [CrossRef] [PubMed]
45. Laha, B.; Stafford, B.; Huberman, A. Regenerating optic pathways from the eye to the brain. *Science* **2017**, *356*, 1031–1034. [CrossRef] [PubMed]
46. Kuffler, D. Can mammalian vision be restored following optic nerve degeneration? *J. Neurorestoratol.* **2016**, *4*, 51–62. [CrossRef]
47. Fujimoto, J.; Breziniski, M.; Tearney, G.; Boppart, S.; Bouma, B.; Hee, M.; Southern, J.; Swanson, E. Optical biopsy and imaging using optical coherence tomography. *Nat. Med.* **1995**, *1*, 970–972. [CrossRef]
48. Momose, K.; New, P.; Grove, A.; Scott, W. The Use of Computed Tomography in Ophthalmology. *Radiology* **1975**, *115*, 361–368. [CrossRef] [PubMed]
49. Alasil, T.; Wang, K.; Keane, P.A.; Lee, H.; Baniasadi, N.; de Boer, J.F.; Chen, T.C. Analysis of normal retinal nerve fiber layer thickness by age, sex, and race using spectral domain optical coherence tomography. *J. Glaucoma* **2013**, *22*, 532–541. [CrossRef]
50. Budenz, D.L.; Chang, R.T.; Huang, X.; Knighton, R.W.; Tielsch, J.M. Reproducibility of retinal nerve fiber thickness measurements using the stratus OCT in normal and glaucomatous eyes. *Investig. Ophthalmol. Vis. Sci.* **2005**, *46*, 2440–2443. [CrossRef] [PubMed]
51. Budenz, D.L.; Fredette, M.J.; Feuer, W.J.; Anderson, D.R. Reproducibility of peripapillary retinal nerve fiber thickness measurements with stratus OCT in glaucomatous eyes. *Ophthalmology* **2008**, *115*, 661–666. [CrossRef] [PubMed]
52. Sony, P.; Sihota, R.; Tewari, H.K.; Venkatesh, P.; Singh, R. Quantification of the retinal nerve fibre layer thickness in normal Indian eyes with optical coherence tomography. *Indian J. Ophthalmol.* **2004**, *52*, 303–309.
53. Frenkel, S.; Morgan, J.E.; Blumenthal, E.Z. Histological measurement of retinal nerve fibre layer thickness. *Eye* **2005**, *19*, 491–498. [CrossRef]
54. Niewiadomska-Kapla, J. Mechanisms of color vision and dyschromatopsi. In *The 25th Symposium of the International Colour Vision Society, Latvia 5–9 July 2019: Book of the Abstract*; Fomins, S., Ozolinsh, M., Eds.; University of Latvia: Riga, Latvia, 2019; p. 78.
55. Kasten, E.; Wüst, S.; Behrens-Baumann, W.; Sabel, B. Computer-based training for the treatment of partial blindness. *Nat. Med.* **1998**, *4*, 1083–1087. [CrossRef]
56. Kasten, E.; Wüst, S.; Sabel, B. Residual Vision in Transition Zones in Patients with Cerebral Blindness. *J. Clin. Exp. Neuropsychol.* **1998**, *20*, 581–598. [CrossRef]
57. Bergandi, L.; Silvagno, F.; Grisolia, G.; Ponzetto, A.; Rapetti, E.; Astori, M.; Vercesi, A.; Lucia, U. The Potential of Visible and Far-Red to Near-Infrared Light in Glaucoma Neuroprotection. *Appl. Sci.* **2021**, *11*, 5872. [CrossRef]
58. Niewiadomska-Kapla, J. *Codici Percettivo del Colore e le Effettive Sensibilità dei Fotorecettori*; Aracne: Roma, Italy, 2018.
59. Bejan, A. *Advanced Engineering Thermodynamics*; Wiley & Sons: New York, NY, USA, 2006.